CrossMark

Synthesis and fluorescence properties of CdTe:Eu^{3+} nanocrystals and core–shell SiO$_2$-coated CdTe:Eu^{3+} nanospheres

Jun-Fang Gao, Jun-Hong Yang, Xiao-Yong Zhang, Jun Zhao, Xing-Wang Liu* ,
Bing-Feng Shi

Abstract Eu^{3+} doped-CdTe (CdTe:Eu^{3+}) nanocrystals were prepared via a facile hydrothermal method, and Eu^{3+} was successfully incorporated into the crystal lattice of CdTe and measured by X-ray powder diffraction (XRD), transmission electron microscopy (TEM), ultraviolet–visible (UV–Vis) absorption spectroscopy and fluorescence emission. The CdTe:Eu^{3+} nanocrystals still have a cubic crystal structure, and the corresponding XRD peaks of CdTe:Eu^{3+} nanocrystals shift to larger angles compared with those of pure CdTe. The CdTe:Eu^{3+} nanocrystals are monodisperse and the particles size is about 2–4 nm. Compared with pure CdTe, the CdTe:Eu^{3+} nanocrystals have larger band gap and thus exhibit blueshift in the emission spectra, which could be accounted for by the energy transfer between Eu^{3+} and CdTe. To enhance the stability and functionality of CdTe:Eu^{3+} nanocrystals, the CdTe:Eu^{3+} nanocrystals were coated with SiO$_2$ and the core–shell SiO$_2$-coated CdTe:Eu^{3+} nanocrystals (CdTe:Eu^{3+}@SiO$_2$) were prepared via microemulsion method. TEM results show that CdTe:Eu^{3+} nanocrystals are uniformly dispersed in the shell, and CdTe:Eu^{3+}@SiO$_2$ nanospheres are uniformly spherical with an average diameter of about 75 nm. The fluorescence emission of CdTe:Eu^{3+}@SiO$_2$ (567 nm) shows a blueshift compared with that of CdTe:Eu^{3+} nanocrystals (632 nm), possibly because of altered surface properties after SiO$_2$ coating. CdTe:Eu^{3+} and CdTe:Eu^{3+}@SiO$_2$ with tunable photoluminescence are potentially useful in fabricating optical and bioimaging devices.

Keywords CdTe:Eu^{3+} nanocrystals; Doping; Core–shell; SiO$_2$; Fluorescent properties

1 Introduction

As a new class of fluorescent materials, semiconductor nanocrystals have attracted much attention due to their potential applications in biological labeling [1–3], electronic and optoelectronic devices [4–6], solar cells [7–9], etc. Introducing dopants can also broaden the range of luminescence than what is achievable with pure materials [10]. Addition of lanthanide ions into semiconductor nanocrystals can often induce dramatic changes in the material's physical and chemical properties and is an efficient way to further enhance its applications [11, 12]. For instance, semiconductor nanocrystals doped with lanthanide ions are capable of efficient luminescence.

CdTe is one of the most typical II–VI semiconductor nanocrystals and it is usually used to prepare nanocrystals that emit red light. The CdTe quantum dots (QDs) can be synthesized by colloidal method [13] or hydrothermal method [14]. The colloidal method is the most popular one to prepare high-quality QDs, but it requires expensive reagents and harsh reaction conditions, and the prepared QDs have a hydrophobic surface and thus cannot be used directly in biological systems. In contrast, hydrothermal synthesis allows the preparation of high-quality QDs at lower temperature, and the resulting QDs are water soluble and thus biocompatible [15].

Lanthanide ions have a unique 4f electronic structure that can introduce novel fluorescence characteristics. The spectral intensity of the trivalent lanthanide ions can be fine-tuned by choosing a suitable medium to embed the ion [16].

J.-F. Gao, J.-H. Yang, X.-Y. Zhang, J. Zhao, X.-W. Liu*
Key Laboratory of Materials Physical Chemistry, Baotou Teachers College, Baotou 014000, China
e-mail: 66090@bttc.edu.cn

B.-F. Shi
Institute of Chemistry, Northeast Normal University, Changchun 130000, China

Lanthanide-doped CdTe-based nanocrystals have been synthesized successfully. Hanifehpour et al. [17, 18] found that doping with Yb^{3+} and Nd^{3+} enhanced the photocatalytic performance of CdTe. Franc et al. [19] characterized the optical and electrical properties of CdTe:Yb nanocrystals co-doped with Ge. Mathew et al. [20] prepared and explored the optical properties of CdTe:Sm^{3+} nanocrystals. However, the synthesis of CdTe:Eu^{3+} nanocrystals remains tedious. It has been reported that the 4f and 5d energy levels of Eu^{3+} can help to promote the growth and crystallization rate of nanocrystals [21], and Eu^{3+} is usually used as an activator of red phosphorus [22]. It remains challenging to incorporate Eu^{3+} dopant into the CdTe host matrix to realize excellent fluorescence properties. Besides, CdTe and doped-CdTe nanocrystals are unstable under harsh environments and can cause cytotoxicity by releasing heavy metal ions from the nanocrystals. To overcome these problems, coating the nanocrystals with a silica shell is a promising method because it can improve the stability and biocompatibility of the material, and because silica is relatively non-toxic. In addition, various functional groups can be readily introduced onto silica shell to enable conjugation with biomolecules [23, 24]. Hence, encapsulating CdTe:Eu^{3+} nanocrystals into SiO_2 shells can help to enhance stability and functionality.

In this work, a facile hydrothermal method to synthesize Eu^{3+} doped-CdTe (CdTe:Eu^{3+}) nanocrystals is presented. CdTe:Eu^{3+} nanocrystals were further coated with SiO_2 via the micro-emulsion method. The microstructures and optical properties of CdTe:Eu^{3+} and core–shell SiO_2-coated CdTe:Eu^{3+} (CdTe:Eu^{3+}@SiO_2) were investigated in detail. The resultant CdTe:Eu^{3+}@SiO_2 shows excellent stability and low cytotoxicity and may find potential use in bioimaging.

2 Experimental

2.1 Materials

Te ($\geq$ 99.99%), $NaBH_4$ ($\geq$ 98%), $CdCl_2 \cdot 2.5H_2O$ ($\geq$ 99%), $Eu(NO_3)_3 \cdot 6H_2O$ ($\geq$ 99.99%), NaOH ($\geq$ 96%) and mer-captopropionic acid (MPA) ($C_3H_6O_2S$) were used as precursor materials in this research.

2.2 Synthesis

2.2.1 Synthesis of CdTe:Eu^{3+} nanocrystals

The NaHTe precursor was prepared as follows: Te powder (1.5 mmol) and $NaBH_4$ (3 mmol) were dispersed in distilled water (5 ml). The mixture was degassed at room temperature and then heated to 50 °C under nitrogen atmosphere with stirring until the Te powder had dissolved completely and the color of the solution turned purple.

The CdTe:Eu^{3+} nanocrystals were prepared by dissolving $CdCl_2 \cdot 2.5H_2O$ (3 mmol), $Eu(NO_3)_3 \cdot 6H_2O$ (0.15 mmol) and MPA (0.63 ml) in distilled water (300 ml) under stirring. This solution was adjusted to pH = 8 with aqueous NaOH (1 mol·L^{-1}) and degassed at room temperature. The NaHTe precursor was then quickly injected under nitrogen atmosphere. The mixture was stirred for several minutes, then transferred into a Teflon reactor and heated at 160 °C. The molar ratio of Cd/Te/MPA was 1.0:0.5:2.4. The resulting nanocrystals were precipitated by ethanol. The crude nanocrystals were dissolved in distilled water and precipitated by ethanol for three cycles, and finally dried under vacuum at 40 °C.

2.2.2 Synthesis of SiO$_2$-coated CdTe:Eu^{3+} nanocrystals

Cyclohexane (75 ml), n-hexyl alcohol (18 ml) and triton X-100 (17.7 ml) was added into a three-necked flask. The mixture was stirred for 20 min to form an inverse emulsion, and the solution of CdTe:Eu^{3+} nanocrystals (10 mg) in distilled water (5 ml) was then added. The mixture was stirred for 20 min before the addition of tetraethoxysilane (TEOS) (0.8 ml), and stirred for another 20 min before the dropwise addition of ammonium hydroxide (0.6 ml). The mixture was finally sealed and allowed to stir at room temperature for 24 h in dark. The resulting nanocrystals were precipitated by acetone, centrifuged, then washed with water and ethanol three times each, and finally dried under vacuum at 40 °C.

2.2.3 Characterization methods

Ultraviolet–Visible (UV–Vis) absorption spectra were recorded on a PE Lambda 950 spectrophotometer (America). Fluorescence emission spectra were obtained with a Horiba JY FluoroLog-3 spectrophotometer using Xe lamp as the excitation source. The concentration of optical analysis is 1 mol·L^{-1}. Transmission electron microscope (TEM) and high-resolution transmission electron microscopy (HRTEM) images were recorded with a JEM-2100 electron microscope at an acceleration voltage of 200 kV. Energy dispersive X-ray spectrometry (EDX) patterns were measured on a PV97-61700ME instrument (America). X-ray powder diffraction (XRD) patterns were measured using a Siemens D-5005 X-ray diffractometer with Cu Kα radiation (0.154 nm).

3 Results and discussion

3.1 Structure and characterization of CdTe:Eu^{3+} nanocrystals

According to XRD patterns in Fig. 1, CdTe and CdTe:Eu^{3+} nanocrystals have the same crystal structure.

CdTe nanocrystals show diffraction peaks at about 24.58°, 40.6° and 47.99°, which very well correspond to (111), (220) and (311) planes of the standard cubic crystal structure of CdTe, respectively. The corresponding peaks of CdTe:Eu^{3+} nanocrystals shift to larger angles. The calculated lattice constants are 0.628 and 0.601 nm for CdTe and CdTe:Eu^{3+} nanocrystals, respectively. These data suggest that Eu^{3+} possibly substitutes Cd^{2+} in CdTe crystal lattice, resulting in the local distortion and shrinkage of the crystal lattice, since Eu^{3+} has a smaller ionic radius (0.095 nm) than Cd^{2+} (0.097 nm) [25]. Eu^{3+} doping into CdTe decreases the lattice constant of CdTe:Eu^{3+} nanocrystals and generates compression stress, which shifts XRD peaks to larger angles [26]. In addition, extra peaks related to any impurity are not observed in CdTe:Eu^{3+}, indicating that phase change does not occur in the CdTe:Eu^{3+} nanocrystals and Eu^{3+} is homogenously distributed within CdTe crystal lattice, as previously demonstrated by Raola and Strouse [27]. The peaks of CdTe:Eu^{3+} nanocrystals are broadened because of the nanosized crystalline domains. The particle size could be calculated by the Scherrer formula:

$$D = K\lambda / \beta \cos\theta \tag{1}$$

where $K = 0.89$ is the Scherrer constant, D (nm) is the diameter of nanocrystals, β is the full width at half maximum (FWHM) of the diffraction peak, θ is the maximum of the diffraction peak and $\lambda = 0.154$ nm is the wavelength of the incident X-ray. The calculated average diameters of the CdTe and CdTe:Eu^{3+} nanocrystals are about 3.4 and 3.1 nm, respectively.

Figure 2 shows TEM and HRTEM images of CdTe:Eu^{3+} nanocrystals harvested after reaction for 10 h. The CdTe:Eu^{3+} nanocrystals appear approximately spherical and dispersed uniformly. The particle diameter is about
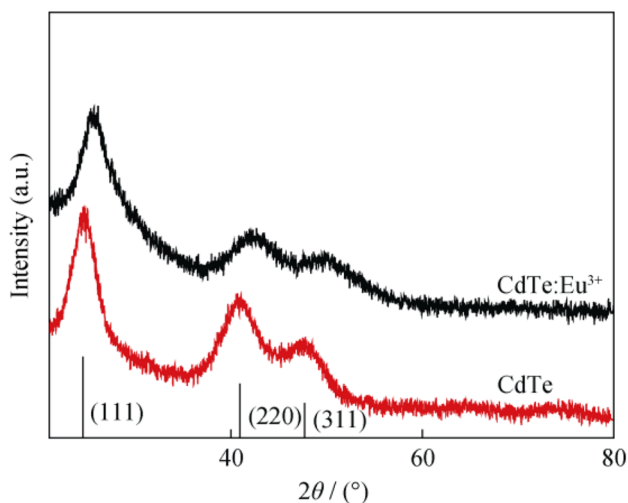

Fig. 1 XRD patterns of CdTe and CdTe:Eu^{3+} nanocrystals

2–4 nm, which is in good agreement with XRD analysis. The lattice distance of CdTe:Eu^{3+} nanocrystals is about 0.33 nm, which is less than the interplanar distance (0.362 nm) of cubic phase CdTe (111). EDX spectrum of CdTe:Eu^{3+} nanocrystals (Fig. 3) shows that Cd, Te and Eu are the elementary components. The atomic ratios of Cd/Te/Eu are found to be 0.689:0.282:0.029. This shows that the elements are basically in their stoichiometry, which proves that the CdTe:Eu^{3+} nanocrystals are successfully prepared.

Figure 4 shows UV–Vis absorption spectra of CdTe and CdTe:Eu^{3+} nanocrystals. The reaction time varies from 6 to 14 h. Compared with pure CdTe nanocrystals at the same reaction time, CdTe:Eu^{3+} nanocrystals show notable blueshift in the absorption spectra. The absorption of the CdTe nanocrystals spans from 492 to 565 nm, and the band gap energy could be calculated as follows:

$$E_g = hc/\lambda \tag{2}$$

where E_g is the photon energy, h is the Planck's constant, c is the speed of light and λ is the edge of absorption. The calculated band gap of CdTe is 2.53–2.20 eV. The absorption of CdTe:Eu^{3+} nanocrystals spans from 477 to 531 nm, and the band gap energy is 2.61–2.34 eV. Note that the CdTe:Eu^{3+} nanocrystals have higher E_g value than the pure CdTe nanocrystals, which shows that doping with Eu^{3+} narrows the band gap of CdTe. Besides, as the reaction time increases, the prepared CdTe:Eu^{3+} nanocrystals gradually show a redshift in the spectra. The relationship between the main absorbance and the size of the nanocrystals is known as follows [28]:

$$D = 9.8127 \times 10^{-7}\lambda^3 - 1.7147 \times 10^{-3}\lambda^2 + 1.0064\lambda \\ - 194.84 \tag{3}$$

where D (nm) is the diameter of the nanocrystals, and λ (nm) represents the wavelength of the UV absorption peak. Accordingly, the average sizes of the CdTe:Eu^{3+} nanocrystals prepared at different reaction time are calculated to be 1.6, 2.2, 2.7, 2.8 and 3.0 nm, respectively. That is, the particle size of the CdTe:Eu^{3+} nanocrystals increases with reaction time, hence resulting in the redshift in the absorption spectra.

Figure 5 shows the luminescence emission spectra of CdTe and CdTe:Eu^{3+} nanocrystals recorded at an excitation wavelength of 376 nm. The emission peaks of CdTe:Eu^{3+} and CdTe nanocrystals are symmetric and show redshift as the reaction proceeds, indicating that the particle size increases with prolonged reaction time. The fluorescent intensity of CdTe nanocrystals increases first and then decreases. However, the fluorescent intensity of CdTe:Eu^{3+} increases after doping with Eu^{3+}, which could be explained as follows. As the reaction proceeds, Cd^{2+} or Eu^{3+} combines with MPA to form Cd-MPA or Eu-MPA complexes, which is adsorbed on the surface of the
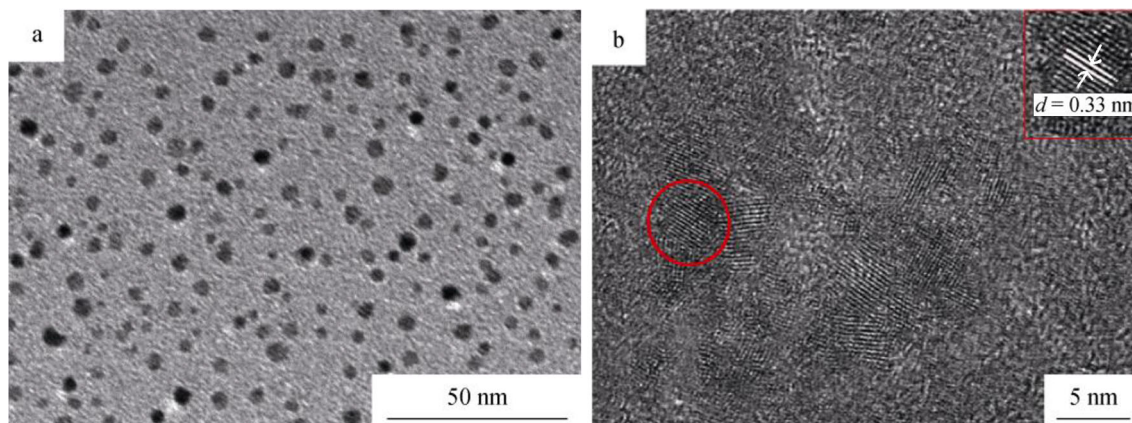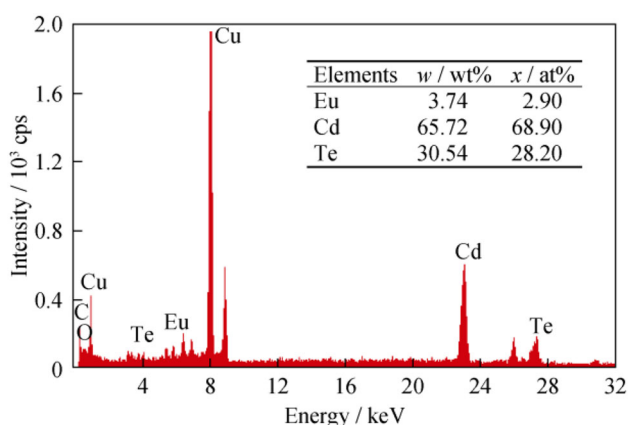
Fig. 2 **a** TEM and **b** HRTEM images of CdTe:Eu^{3+} nanocrystals

Fig. 3 EDX analysis of CdTe:Eu^{3+} nanocrystals

Elements	w / wt%	x / at%
Eu	3.74	2.90
Cd	65.72	68.90
Te	30.54	28.20

nanocrystals and prevents the aggregation of nanocrystals. When the reaction time exceeds 10 h, the fluorescence intensity of CdTe decreases, because the particle size increases further whereas the amount of Cd-MPA complexes decreases. Consequently, the CdTe nanocrystals are aggregated, which decreases the fluorescence intensity.

However, the intensity of CdTe:Eu^{3+} still increases, which could be attributed to the effect of doping. When Eu^{3+} are doped into CdTe, defect states are introduced near the surface regions and hence they give better emission efficiencies [29]. Besides, the FWHM of the fluorescence spectrum increases with reaction time, indicating that the size distribution of the nanocrystals broadens, possibly due to Ostwald ripening.

The emission peaks of CdTe nanocrystals range in 541–628 nm, whereas those of CdTe:Eu^{3+} nanocrystals range in 532–602 nm. The emission peaks of CdTe:Eu^{3+} exhibit a blueshift compared with undoped CdTe nanocrystals prepared at the same reaction time. That is, a maximum blueshift of about 39 nm is observed between emission peaks of CdTe nanocrystals (599 nm) and that of CdTe:Eu^{3+} nanocrystals (560 nm) both prepared at a reaction time 10 h. It could be inferred that Eu^{3+} are doped into the lattice of the CdTe nanocrystals and the energy may be transferred from host CdTe to Eu^{3+} [30]. This may be explained by the energy level diagram (Fig. 6). Upon excitation of CdTe:Eu^{3+} nanocrystals by 376 nm, after absorbing an excitation photon, the electron in the valence
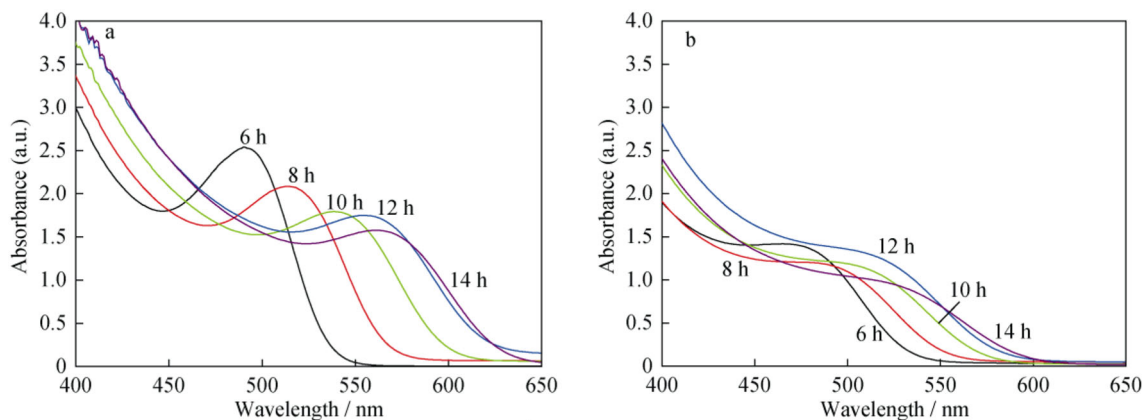

Fig. 4 UV–Vis absorption spectra of **a** CdTe and **b** CdTe:Eu^{3+} nanocrystals at different reaction time
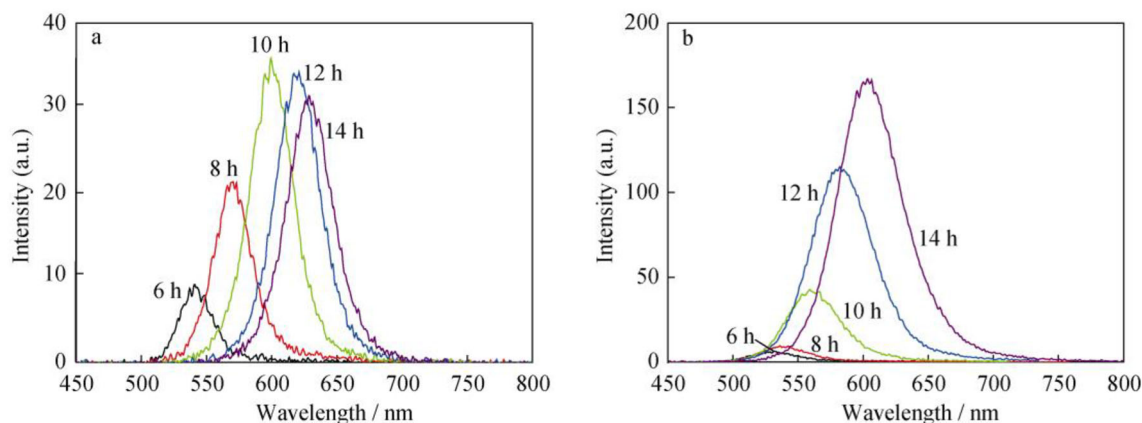
Fig. 5 Fluorescence emission spectra of **a** CdTe and **b** CdTe:Eu^{3+} nanocrystals at excitation wavelength of 376 nm

band of CdTe nanocrystals is excited into the conduction band. An exciton pair consisting of the electron and the positively charged hole is formed and traveled through the CdTe nanocrystal lattice. The exciton pair could be trapped at defect sites in the lattice, such as Eu^{3+} substitution, transfer non-radiatively to $^5D_4$ and further to $^5D_0$, then radiative transitions from $^5D_0$ of Eu^{3+} to various ^7F_J ($J = 0$–6) levels. The energy could be transferred from CdTe host to Eu^{3+} [31].

3.2 Structure and fluorescence of core–shell SiO$_2$-coated CdTe:Eu^{3+} nanocrystals

To enhance the functionality and optical stability of CdTe:Eu^{3+} nanocrystals, core–shell SiO$_2$-coated CdTe:Eu^{3+} nanospheres (CdTe:Eu^{3+}@SiO$_2$) were synthesized via micro-emulsion method. The surface defects of

CdTe:Eu^{3+} nanocrystals could be reduced after SiO$_2$ coating. Consequently, the emission spectra of CdTe:Eu^{3+}@SiO$_2$ nanospheres show further blueshift and stronger fluorescence intensity.

Figure 7 shows XRD patterns of CdTe and CdTe:Eu^{3+}@SiO$_2$ nanospheres. The peak at 22.8° could be attributed to amorphous SiO$_2$. The peak at 40.6° corresponds to the characteristic CdTe:Eu^{3+} (220) crystal planes, which proves that CdTe:Eu^{3+} enters SiO$_2$ shell successfully.

Figure 8 shows TEM image of CdTe:Eu^{3+} and CdTe:Eu^{3+}@SiO$_2$, in which the core–shell structure can be clearly distinguished. Note that CdTe:Eu^{3+}@SiO$_2$ ($\sim$ 75 nm in size) appears spherical, monodisperse and without aggregation. HRTEM images of CdTe:Eu^{3+}@SiO$_2$ nucleus are shown in the upper right corner (Fig. 8b). The particle size of the nucleus is about 3.6 nm, and the lattice distance is 0.33 nm, which is consistent with the CdTe:Eu^{3+} nanocrystals (Fig. 2). This indicates that CdTe:Eu^{3+} is successfully embedded into SiO$_2$ shell.
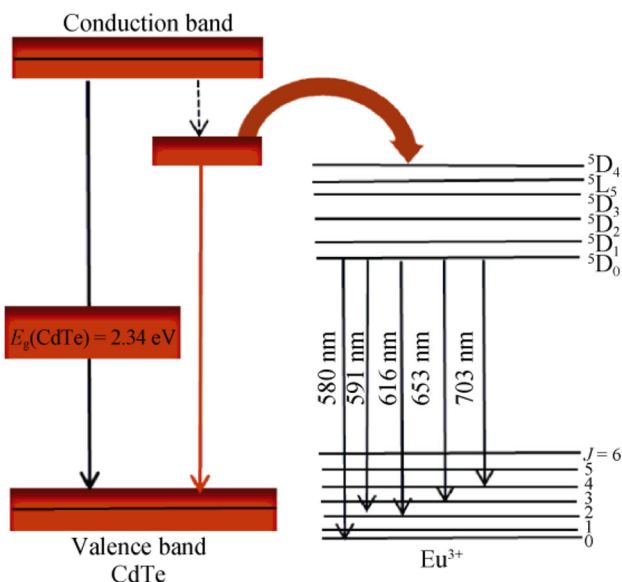

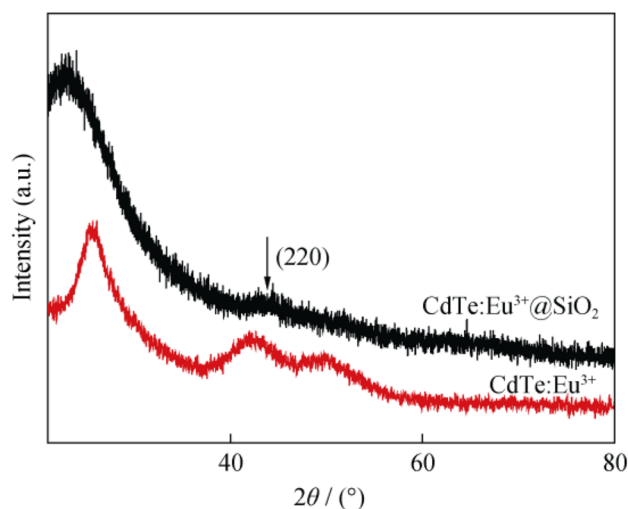**Fig. 6** Schematic of energy transfer process from CdTe to Eu^{3+}

Fig. 7 XRD patterns of CdTe:Eu^{3+} nanocrystals and CdTe:Eu^{3+}@SiO$_2$ nanospheres
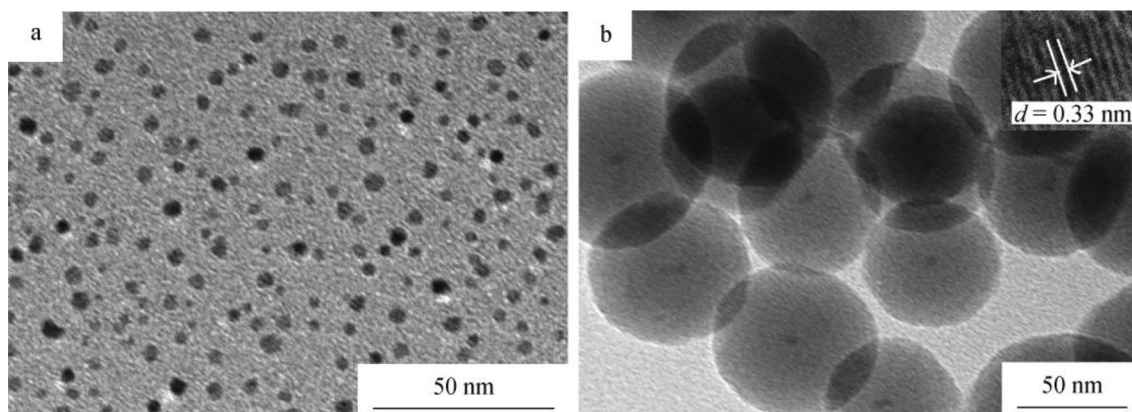
Fig. 8 TEM images of **a** CdTe:Eu^{3+} nanocrystals and **b** CdTe:Eu^{3+}@SiO$_2$ nanospheres

Figure 9 shows the emission spectra of both CdTe:Eu^{3+} nanocrystals and core–shell SiO$_2$-coated CdTe:Eu^{3+} nanocrystals at an excitation wavelength of 376 nm. The fluorescent emission of CdTe:Eu^{3+} centers at 632 nm, whereas the emission of CdTe:Eu^{3+}@SiO$_2$ nanospheres centers at 567 nm. This blueshift of 65 nm from CdTe:Eu^{3+} to CdTe:Eu^{3+}@SiO$_2$ indicates that coating with SiO$_2$ changes the surface structure and fluorescence properties of CdTe:Eu^{3+} nanocrystals. Specifically, a large number of MPA fall off from the surface of CdTe:Eu^{3+} nanocrystals during cladding, leading to the oxidation of CdTe:Eu^{3+} nanocrystals and consequently the blueshift of the emission peaks of CdTe:Eu^{3+}@SiO$_2$ [32]. The stronger fluorescence intensity of CdTe:Eu^{3+}@SiO$_2$ nanospheres could be rationalized as follows. In the core–shell SiO$_2$-coated CdTe:Eu^{3+}, the hole is confined within CdTe:Eu^{3+} core, whereas the electron is delocalized over the entire sphere, and SiO$_2$ could stop the electron–hole recombination on the CdTe:Eu^{3+} surface. These altogether reduce non-radiative transition and permitted electrical access to the sphere, thus improving the emission intensity [33].
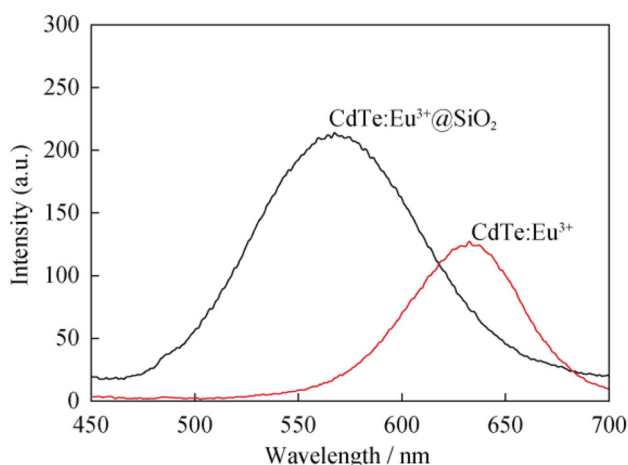

Fig. 9 Emission spectra of CdTe:Eu^{3+}@SiO$_2$ and CdTe:Eu^{3+} nanocrystals

4 Conclusion

Highly fluorescent CdTe:Eu^{3+} nanocrystals were synthesized via a hydrothermal method, and their structure, shape, elemental composition and fluorescence properties were investigated. Results indicate that Eu^{3+} is successfully doped into the lattice of CdTe nanocrystals. Compared with CdTe, CdTe:Eu^{3+} nanocrystals show blue shift in both absorption spectra and emission spectra, which possibly results from the energy transfer between Eu^{3+} and CdTe. The possible energy transfer mechanism between Eu and CdTe nanocrystals is also studied. In addition, the obtained CdTe:Eu^{3+} nanocrystals were coated with SiO$_2$ to fabricate core–shell SiO$_2$-coated CdTe:Eu^{3+} (CdTe:Eu^{3+}@SiO$_2$) nanospheres via the micro-emulsion method. Compared with CdTe:Eu^{3+} nanocrystals, CdTe:Eu^{3+}@SiO$_2$ nanospheres exhibit further blueshift and stronger fluorescence intensity. Our strategy provides a facile process for the preparation of lanthanide ion doped nanocrystals and their SiO$_2$-coated core–shell. The obtained lanthanide ion doped nanocrystals and fluorescent core–shell nanospheres are potentially useful in fabricating multifunctional optoelectronic devices and bioimaging.

References

[1] Huang HQ, Liu JL, Han BF, Mi CC, Xu SK. Cell labeling and cytotoxicity of aqueously synthesized CdTe/CdS/ZnS core–shell–shell quantum dots by a water bath-hydrothermal method. J Lumin. 2012;132(4):1003.

[2] Liu P, Wang Q, Li X. Studies on CdSe/L-cysteine quantum dots synthesized in aqueous solution for biological labeling. J Phys Chem C. 2009;113:7670.

[3] Kumar R, Nyk M, Ohulchanskyy TY, Flask CA, Prasad PN. Combined optical and MR bioimaging using rare earth ion doped NaYF$_4$ nanocrystals. Adv Funct Mater. 2009;19(111): 853.

[4] Jiang ZY, Zhu KR, Lin ZQ, Jin SW, Li G. Structure and Raman scattering of Mg-doped ZnO nanoparticles prepared by sol–gel method. Rare Met. 2018;37(10):881.

[5] Jin H, Wang YY, Wang YT, Yang HB. Synthesis and properties of electrodeposited Ni–CeO$_2$ nano-composite coatings. Rare Met. 2018;37(2):148.

[6] Han X, Zhang JM, Zhang K, Wang TY. Synthesis and modification of water-soluble CdTe: Zn quantum dots. Chin J Rare Met. 2015;39(10):909.

[7] Zebardastan N, Khanmirzaei MH, Ramesh S, Ramesh K. Performance enhancement of poly (vinylidene fluoride-co-hexafluoro propylene)/polyethylene oxide based nanocomposite polymer electrolyte with ZnO nanofiller for dye-sensitized solar cell. Org Electron. 2017;49:292.

[8] An QZ, Fassl P, Hofstetter YJ, Becker-Koch D, Bausch A, Hopkinson PE, Vaynzof Y. High performance planar perovskite solar cells by ZnO electron transport layer engineering. Nano Energy. 2017;39:400.

[9] Yu JJ, Liao B, Zhang X. Fabrication of 3D ZnO/CuO nanotrees and investigation of their photoelectrochemical properties. Chin J Rare Met. 2018;42(5):450.

[10] Buonsanti R, Milliron D. Chemistry of doped colloidal nanocrystals. Chem Mater. 2013;25(8):1305.

[11] Ishizumi A, Taguchi Y, Yamamoto A, Kanemitsu Y. Luminescence properties of ZnO and Eu^{3+}-doped ZnO nanorods. Thin Solid Films. 2005;486(1–2):50.

[12] Zhang WJ, Li Y, Zhang H, Zhou XG, Zhong XH. Facile synthesis of highly luminescent Mn-doped ZnS nanocrystals. Inorg Chem. 2011;50(20):10432.

[13] Murray CB, Norris DJ, Bawendi MG, Murray CB, Norris DJ, Bawendi MG. Synthesis and characterization of nearly monodisperse CdE (E = S, Se, Te) semiconductor nanocrystallites. J Am Chem Soc. 1993;15(19):8706.

[14] Zhang H, Wang LP, Xiong HM, Hu LH, Yang B, Li W. Hydrothermal synthesis to high quality CdTe nanocrystals. Adv Mater. 2003;15(20):1712.

[15] Wang Q, Zhou XL, Fang TT, Liu P, Li X, Min XM. One-step growth of high-quality CdTe quantum dots via hydrothermal method and cytotoxicity evaluation. Powder Technol. 2013;247: 81.

[16] Nogami M. Fluorescence properties of Eu-doped GeO$_2$–SiO$_2$ glass heated under an H$_2$ atmosphere. Lumin. 2001;92(4):329.

[17] Hamnabard N, Hanifehpour Y, Khomami B, Joo SW. Synthesis, characterization and photocatalytic performance of Yb-doped CdTe nanoparticles. Mater Lett. 2015;145:253.

[18] Hanifehpour Y, Hamnabard N, Khomami B, Joo SW, Min BK. A novel visible-light Nd-doped CdTe photocatalyst for degradation of Reactive Red 43: synthesis, characterization, and photocatalytic properties. J Rare Earths. 2016;34(1):46.

[19] Franc J, Horodysky P, Grill R, Kubat J, Saucedo E, Sochinskii NV. Characterization of optical and electrical properties of CdTe: Yb co-doped with Ge. J Cryst Growth. 2006;286(2):384.

[20] Mathew S, Rejikumar PR, Adiyodi AK, Jyothy PV, Unnikrishnan NV. Structural and optical characterization of oxygenated CdTe/Sm^{3+} in sol–gel silica glasses. Mater Chem Phys. 2008; 112(3):1061.

[21] Zhu YS, Cui SB, Chen X, Xu W, Zhou PW, Wang YF, Xu L, Song HW, Huang L, Huang W. Efficient energy transfer from inserted CdTe nanocrystals to YVO4:Eu^{3+} inverseopals: a novel strategy to improve and expand visible excitation of rare earth ions. Nanoscale. 2014;6(14):8075.

[22] Xu HY, Zhang JH, Li FS. Synthesis and optical properties of CdTe:Eu^{3+} quantum dots. Chin J Lumin. 2016;37(3):306.

[23] Yang YH, Gao MY. Preparation of fluorescent SiO$_2$ particles with single CdTe nanocrystal cores by the reverse microemulsion method. Adv Mater. 2005;17(19):2354.

[24] Zhang SH, Wen L, Yang JP, Zeng JF, Sun Q, Li Z, Zhao DY, Dou SX. Facile fabrication of dendritic mesoporous SiO$_2$@CdTe@SiO$_2$ fluorescent nanoparticles for bioimaging. Part Part Syst Charact. 2016;33(5):261.

[25] Zhang Y, Liu Y, Li X, Wang QJ, Xie E. Room temperature enhanced red emission from novel Eu^{3+} doped ZnO nanocrystals uniformly dispersed in nanofibers. Nanotechnology. 2011; 22(41):415702.

[26] Park JY, Jeong DW, Lim KM. Multimodal luminescence properties of surface-treated ZnSe quantum dots by Eu. Appl Surf Sci. 2017;415:8.

[27] Raola OE, Strouse GF. Synthesis and characterization of Eu-doped cadmium selenide nanocrystals. Nano Lett. 2002;2(2): 1443.

[28] Chen YF, Chen Z, He YJ, Lin HL, Sheng PT, Liu CB, Luo SL, Cai QY. L-cysteine-capped CdTe QD-based sensor for simple and selective detection of trinitrotoluene. Nano-technology. 2010;21(12):125502.

[29] Ashwini K, Yashaswinia B, Pandurangappa C. Solvothermal synthesis, characterization and photoluminescence studies of ZnS:Eu nanocrystals. Opt Mater. 2014;37:537.

[30] Kabongo GL, Mhlongo GH, Malwela T, Mothudi BM, Hillie KT, Dhlamini MS. Microstructural and photoluminescence properties of sol–gel derived Tb^{3+} doped ZnO nanocrystals. J Alloys Compd. 2014;591:156.

[31] Luo WQ, Liu YS, Chen XY. Lanthanide-doped semiconductor nanocrystals: electronic structures and optical properties. Sci China Mater. 2015;58(10):819.

[32] Ning ZD, Zhang JM, Wei J, Cheng YY. CdTe@SiO$_2$ particles prepared via reverse microemulsion method and its fluorescence properties. J Tianjin Polytech Univ. 2012;31(1):50.

[33] Song HY, Leem YM, Kim BG, Yu YT. SiO$_2$-coated ZnS submicrospheres with enhanced thermal stability and photoluminescence. Mater Sci Eng. 2007;B143:70.